A Model for Probability Nowcasts of Accumulated Precipitation Using Radar

TAGE ANDERSSON AND KARL-IVAR IVARSSON

Swedish Meteorological and Hydrological Institute, Norrköping, Sweden

(Manuscript received 9 January 1990, in final form 30 May 1990)

ABSTRACT

A new model for making probability forecasts of accumulated spot precipitation from weather radar data is presented. The model selects a source region upwind of the forecast spot. All pixels (horizontal size 2×2 km^2) within the source region are considered, having the same probability of hitting the forecast spot. A pixel hitting the forecast spot is supposed to precipitate there a short time (about 10 min.). A drawing is performed, and a frequency distribution of accumulated precipitation during the first time step of the forecast is obtained. A second drawing gives the frequency distribution of accumulated precipitation during the first to second time step, a third one during the first to third, and so on until the end of the forecast period is reached. A number of forecasts for 1-h accumulated precipitation, with lead times of 0, 1, and 2 h, have been performed and verified. The forecasts for 0-h lead time got the highest Brier skill scores, +50% to 60% relative to climatological forecasts for accumulated precipitation below 1 mm.

1. Introduction

At present a main operative use of weather radar is subjective nowcasting of precipitation. Even forecasts of accumulated precipitation are often made subjectively, though there are numerical methods (Austin et al. 1986; Carpenter and Owens 1981; Walton and Johnson 1986; Einfalt et al. 1989). These models give categorical answers and are mainly advective.

The main difficulty is the rapid changes with time of the echoes. In our area the average lifetime of a shower is 16 min with a standard deviation of 8 min (Wickerts 1982). Of course the "lifetime" depends upon the definition used. However, attempts of tracking such short-lived phenomena for time periods on the order of hours are futile. Even for nonconvective precipitation the echoes change rapidly. Since at present there are no operative models capable of forecasting the development of precipitating cells on this scale, the development of a probabilistic model is natural. Such a model is described by Zuckerberg (1976). Building upon the Poisson distribution it, however, only gives the probability of rain/no rain.

In the present work an advective model, first described by Andersson (1989), is developed and verified. It gives the probability of accumulated spot precipitation. An area (the source area) upwind of the forecasting spot is advected over the spot. The 850-hPa forecasted wind has been used, but a wind measured by the radar itself or the estimated echo movement may be used. Showers in this area usually move with the 850-hPa wind (Wickerts 1982). The frequency distribution of reflectivities within this area is then computed. The class limits are selected so that there is a doubling of the rainrate for every class increment. The horizontal resolution is 2 km. Using a predefined rainrate–reflectivity relation, the distribution of accumulated precipitation during a small time interval, the time step, is computed. In the source region the reflectivities are assumed to be randomly distributed. During the advection all pixels within the source region have equal probabilities of hitting the forecast spot. That is, we consider the areal frequency distribution of reflectivities as the point frequency distribution. For every time step a drawing is made. The drawings depict the frequency distribution of accumulated precipitation for the first time step, the first to the second, the first to the third, . . . , the first to the last one, which is the forecasted probability distribution of accumulated precipitation.

2. Method

a. Geometry

The geometry is shown in Fig. 1. A source area upwind of the forecasting spot is selected. The 850-hPa wind according to the latest forecast from the Swedish limited area model (Gustafsson and Törnevik 1984) is selected as steering wind. Since the radar (the Ericsson *C*-band Doppler weather radar in Norrköping) has Doppler capability it is, however, possible to use the actual wind according to the radar. The wind at a proper level may be obtained from manual interpretation of the radial winds on the PPI (plan projection indicator), or from automatic interpretations as ve-

Corresponding author address: Dr. Tage Andersson, Swedish Meteorological and Hydrological Institute, 601 76 Norrköping, Sweden.

locity azimuth display or uniform wind technique (Persson and Andersson 1987). It is also possible to estimate the echo movement from comparisons between two consecutive echo images. Though this idea seems very attractive, there are occasions when the echoes do not move with the wind at any level, this is a very difficult task. The reason is that the echoes are always changing and there is usually no way to decide whether the observed changes between two consecutive echo images are due to echo movement or echo growth/decay. Therefore, we have considered the use of the forecasted wind at a proper level, the best method to obtain the echo movement.

Denoting the wind speed ff, the radius of the source area is $ff \times$ (forecast time duration)/2 or, if this is below a minimum value, the minimum value (selected as 20 km). To produce a forecast at least half the source region shall be within the range of the radar. The reason for choosing this radius is that during the forecast period a distance $ff \times$ (forecast time duration) is advected over the forecast spot. Assuming,

- the pixels do not change reflectivity with time,
- they move with the 850-hPa wind, and
- there is a unique and exact relation between reflectivity and rainrate,

one only has to compute the precipitation over the forecast spot from each pixel passing it. However, none of these conditions is fulfilled. Therefore we have introduced the concept "source area" and assume that even if the pixels rapidly change their reflectivity, the reflectivity distribution within the source area remains constant, and that the pixels within that area have equal probabilities of hitting the forecast spot.

b. *Frequency distributions*

The equivalent radar reflectivity factor, hereafter called reflectivity, and given in dBZ, is the main parameter. Its frequency distribution within the source area is computed. For practical reasons a minimum dBZ value has to be selected. Reflectivities below this value are considered to give rainrate zero. The class width is selected so that the rainfall rate increases with a factor of 2 for every class increment. The class width is then dependent upon the reflectivity–rainrate relation used. With the relation used by us,

$$Z = 430R^{2.0} \qquad (1)$$

the class width becomes 6.0 dBZ. (Z = factor of reflectivity mm^6 m^{-3}, R = rainrate mm h^{-1}.)

The choice of this relation needs some comment. In the literature a coefficient as high (or higher than) 2.0 is only given for (melting) snow. We have, however, found that using lower values of that coefficient gives unreasonably high accumulated precipitation in the cores of showers, (i.e., where reflectivities are high). The relation gives reasonable accumulated precipitation sums also for low and moderate rain. (This may be a peculiarity for our radar).

We have chosen eight classes, the class 0 giving rainrate = 0 and class 7 rainrate = 64 mm h^{-1} (class midpoint), see Table 1. We then have the frequency distribution of reflectivities

$$f\_\mathrm{dBZ}(\mathrm{cl})$$

where cl is the class number, and each cl corresponds to a rainrate R (mm h^{-1}).

We can also let cl correspond to an accumulation during the time step. The accumulated rain is then

$$\mathrm{acc} = R \times \text{time step}, \qquad (2)$$

and we get the frequency distribution

$$f\_\mathrm{step}(\mathrm{cl}).$$

For instance, if the time step = 10 min, cl = 3 corresponds to $4 \times 10/60 = 0.7$ mm.

At the forecast spot the frequency distribution of accumulated rain is denoted

$$f\_\mathrm{acc}(t, \mathrm{acc})$$

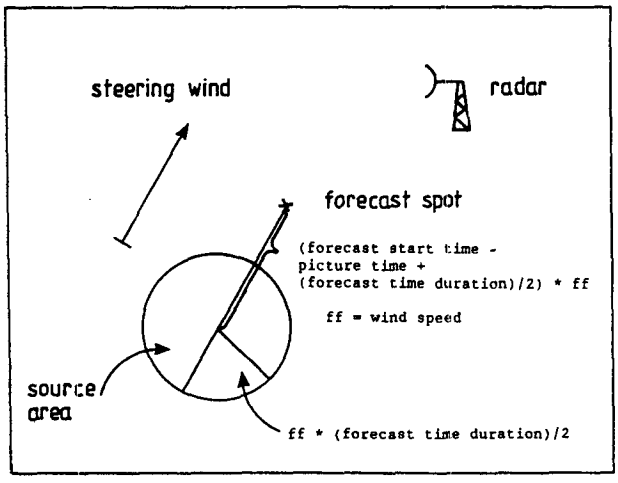

FIG. 1. Forecast "geometry" and definition of the source area. The area has a minimum radius, see text.

TABLE 1. Classification of reflectivities (class midpoints) and associated rain rates. Reflectivities <23.3 dBZ are considered to give rainrate = 0.0 mm h^{-1}.

cl	Z dBZ	R mm h^{-1}
0	20.3	0.0
1	26.3	1.0
2	32.4	2.0
3	38.4	4.0
4	44.4	8.0
5	50.4	16.0
6	56.4	32.0
7	62.4	64.0

where t is the number of time steps, and acc is the accumulated rain with a resolution of 0.1 mm. In practice we work with this as a one-dimensional array, since only the result from the last time step is saved. For the time step we have selected 10 min.

c. Computing the expected frequencies of accumulated precipitation

At the start ($t = 0$), $f\_\text{acc}(0, 0) = 1.0$, and $f\_\text{acc}(0, x) = 0.0$ where $x > 0$; i.e., there is then no accumulated rain. The method, for a case of two classes and three drawings, is shown by Fig. 2. After a drawing

$$f\_\text{acc}(t + 1, \text{acc} + \text{cl}) = \sum_{\text{cl}=0}^{7} \sum_{\text{acc}=0}^{\max} f\_\text{acc}(t, \text{acc}) \times f\_\text{step}(\text{cl}). \quad (3)$$

Note that different combinations of acc and cl may result in the same (acc + cl). The upper limit max is the maximum accumulated precipitation expected. It has to be selected considering the forecast's time duration and the climate type. We have used max = 30 mm for a forecast time duration of 1 h. This is then repeated until the end of the forecast period is reached. If it were possible to forecast the development of the rain, $f\_\text{step}(\text{cl})$ could be a function of time. At present, however, we do not see any possibilities for this, except perhaps for summer showers that over land often have a pronounced daily march.

3. Forecasts tested

Several forecast lengths and start times may be selected and several parameters may be displayed. We have tested forecasts of 1-h accumulated precipitation, starting at three different times:

(i) radar image time + 0 h

(ii) radar image time + 1 h

(iii) radar image time + 2 h

The forecasts may be displayed as probabilities for different spot rain amounts as in Table 2.

The forecast spots used, as are shown in Fig. 3, are such with recording raingages (resolution 0.1 mm) that the forecasts may be verified against conventional gage measurements.

4. Verification

We have verified forecasts from six rains during 24 August to 23 October 1989. If the forecasts are rounded to the nearest 10% probability (0, 10, 20, . . . , 100%) and interpreted as probabilistic (Murphy and Katz 1985) we get Table 3. The reliability (Murphy and Katz 1985) is a measure of the degree of correspondence between the forecasted probability and the corresponding observed relative frequency.

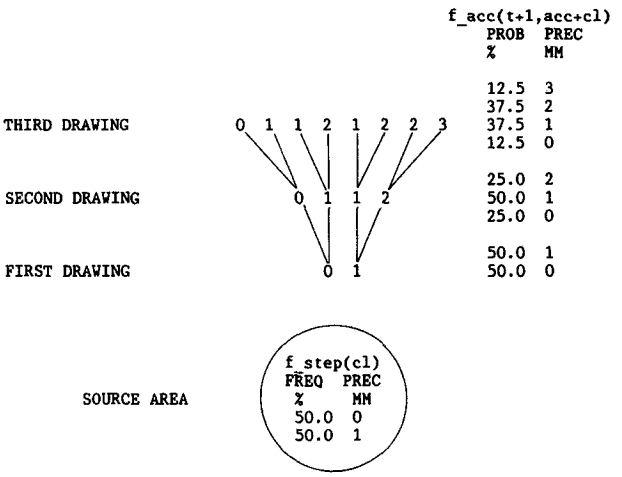

FIG. 2. The method of drawing. A case with two classes and three drawings.

$$\text{REL} = \sum_{i=1}^{N} (f_i - p_i)^2 / N \quad (4)$$

N = number of subsamples; i.e., the number of different forecast probabilities (here 0%, 10%, 20%, . . . , 100%; i.e., 11 or less); f = observed relative frequency when the forecast probability p is given.

The forecasts with the shortest lead time have the highest reliability, as shown in Table 3. Note that a high reliability corresponds to a low numerical value. There is a tendency for underforecasting all probabilities except for 0-h lead time and rain amounts <1 mm. In spite of this, examination of the complete material underlying Table 3 shows a slight tendency of too "self confident" forecasts for longer lead times, meaning an underforecasting for low probability values and an overforecasting for high ones. This is often the case for forecasts (Murphy and Daan 1984; Ivarsson et al. 1986).

The overall bias is low with a slight underforecasting that, however, is increasing with the lead time. The most important contributing factor to this increase is certainly overshooting of the beam. With high wind speed, the source area for some of the verification spots (which are surrounding the radar in all directions) will be situated at a long distance from the radar. However, the observed frequencies decrease with the lead time. This must be due to the selection of test situations. A probable reason is an instinctive bias towards cases with precipitation in the proximity of the radar. If so, this may also contribute to the underforecasting.

The resolution (Murphy and Katz 1985) in this context is a measure of the ability to resolve the future weather into situations with high frequencies and low frequencies of (in this case) rain. In other words, resolution relates to the extent to which different forecasts are followed by different observations.

TABLE 2. Forecast probabilities of at least the given amounts of 1 h accumulated precipitation (unit 0.1 mm) for 10 stations, see Fig. 3. VER gives the actual precipitation according to conventional, telemetering gauges of the tipping bucket type. 999 means no measurement. Radar image time: 1703 UTC 3 Nov 1989. The advecting wind was 172°/25 kt. For forecast start +2 h the source area center for stations 722 and 733 was about 200 km from the radar antenna, and the beam was certainly overshooting most of the precipitation.

Forecast start = image time + 0.0 h. Forecast length 1.0 h

Probability (%)	P700	P708	P719	P721	P722	P723	P724	P729	P732	P733
100	0	0	0	6	0	2	0	0	0	0
90	0	0	0	17	4	7	2	0	0	2
80	0	0	0	21	7	10	3	0	0	3
70	0	0	0	25	10	12	4	1	0	5
60	0	0	0	28	13	14	5	1	1	7
50	1	0	0	32	16	17	6	2	1	8
40	1	0	0	36	20	19	7	3	3	10
30	2	0	0	40	25	22	8	3	4	12
20	3	0	0	46	31	26	10	4	7	15
10	3	0	0	53	40	33	13	7	11	18
VER	0	0	0	22	17	2	8	1	0	1

Forecast start = image time + 1.0 h. Forecast length 1.0 h

Probability (%)	P700	P708	P719	P721	P722	P723	P724	P729	P732	P733
100	0	0	0	0	0	0	0	0	2	0
90	2	0	0	0	0	0	0	0	8	4
80	3	0	0	0	0	0	0	1	10	6
70	5	0	0	0	0	1	0	1	12	7
60	7	0	0	1	1	1	3	2	14	8
50	9	0	0	1	1	2	3	3	15	9
40	12	1	0	2	2	3	4	4	17	11
30	15	1	0	3	3	3	5	5	19	12
20	18	2	0	4	4	5	7	7	22	14
10	27	3	0	7	6	8	9	9	26	17
VER	20	4	0	14	2	12	18	8	17	11

Forecast start = image time + 2.0 h. Forecast length 1.0 h

Probability (%)	P700	P708	P719	P721	P722	P723	P724	P729	P732	P733
100	0	0	0	0	0	0	0	0	0	0
90	4	2	0	0	0	0	0	0	1	0
80	6	4	0	1	0	1	0	0	2	0
70	8	6	0	1	0	1	0	0	3	0
60	10	8	0	2	0	2	0	0	4	0
50	11	11	0	3	0	3	1	0	5	0
40	13	14	0	3	0	3	1	0	6	0
30	15	16	0	4	0	4	3	0	7	0
20	18	21	0	5	0	5	3	0	8	0
10	22	28	0	7	0	7	6	0	10	0
VER	25	26	3	2	6	4	13	22	15	14

$$\mathrm{RES} = \sum_{i=1}^{N} (f_i - c)^2/N, \qquad (5)$$

c = the rounded sample climatology (Murphy and Katz 1985). The sample climatology is frequency given by the actual sample. If for instance that frequency is 0.321 the rounded one is 0.3. The resolution is highest for the lowest lead times and the lowest rain sums, reflecting the fact that it is most difficult to forecast intense rains for long lead times.

The skill is the Brier skill score (Brier 1950; Murphy and Katz 1985) when the reference forecast is the rounded sample climatology.

$$\mathrm{SKILL} = 100 \times (\mathrm{BC} - \mathrm{BR})/\mathrm{BR}, \qquad (6)$$

BC = Brier score from rounded sample climatology; BC = $F \times (F - 1)$ + DIFF; F = sample climatology (not rounded); DIFF = square difference between rounded and not rounded relative frequency; BR = Brier score from radar forecasts. Note that BR = BC

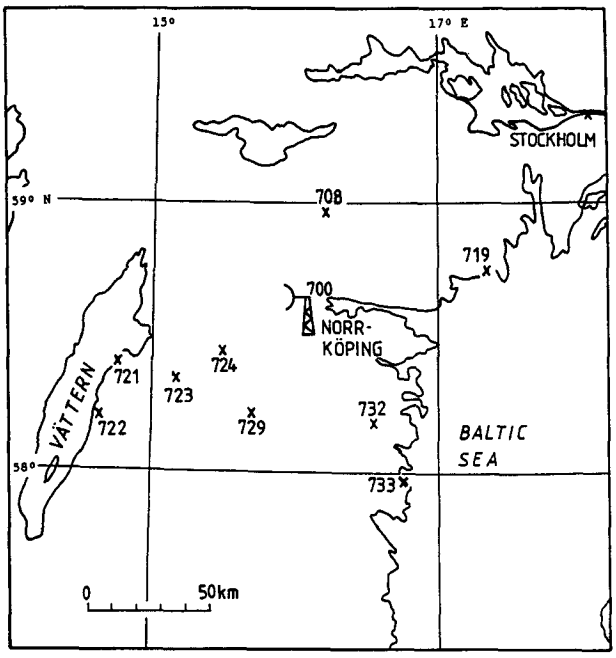

FIG. 3. Map of the investigation area, showing the positions of the radar and stations used for verification of the forecasts.

+ REL − RES. The skill is very high for the forecasts having the shortest lead time especially if the forecast rain sum is not too large (low threshold value). A graphical picture of these parameters and an example of how the forecasts work is given by the reliability diagram of Fig. 4. However, since all forecasts have very short lead times it may be more interesting to compare them with the climatological expected probabilities (i.e., the relative frequencies given by climatological statistics) based on the state of weather when the forecast is made; i.e., the image time. This climatological expected probability is a kind of persistency probability forecast. As an example, suppose that the conditional probability of rain during period 1 is 60% if there is rain during period 0, but is 10% if there is not rain during period 0. The persistency forecasts then use these probabilities. For this case it may be shown that the autocorrelation is 0.50 and the unconditional probability of rain is 20%. The climatological forecasts use this probability. Since persistence forecasts perform better than climatological ones, using persistency as reference gives lower skills.

The autocorrelation for rain (period duration 1 h, summer climate in southern Sweden) is about 0.7 and can be used as an approximation for hourly rain ≥ 0.1 mm. If the Markov property (for explanation of the Markov property see Cox et al. 1980) is assumed it can be shown that the autocorrelation for rain, periods 0–1 h to 1–2 h will be $0.7^2 = 0.49$ and the corresponding figure for periods 0–1 h to 2–3 h will be $0.7^3 = 0.34$.

It can also be shown that the Brier skill score using persistency probability forecasts is the square of the autocorrelation. (If the reference forecast is assumed to be the climatology and the climatological probability is constant from 1 h to another). Table 4 gives the results for rain ≥ 0.1 mm.

However the result implies that up to 2 h lead time the forecasts give more valuable information than pure persistency forecasts do (alone). It must also be noted

TABLE 3. Results from verification of forecasts from six rains during 24 August–23 October 1989. Threshold gives threshold values of 1-h accumulated precipitation. For explanation of other terms, see text.

Threshold (mm)	Forecast frequency	Observed frequency	Number of forecasts	Reliability	Resolution	Skill score	Brier score
			0 h lead time				
0.1	49.5%	51.8%	369	0.0065	0.1557	59.7%	0.1007
0.3	41.7%	41.2%	369	0.0123	0.1599	60.9%	0.0947
0.5	32.9%	33.3%	369	0.0021	0.1260	55.5%	0.0994
1.0	20.0%	23.0%	369	0.0068	0.0967	50.4%	0.0883
2.0	5.8%	8.7%	369	0.0075	0.0224	18.8%	0.0644
			1-h lead time				
0.1	43.2%	47.8%	370	0.0172	0.1123	38.0%	0.1549
0.3	35.1%	37.3%	370	0.0230	0.0853	26.6%	0.1723
0.5	26.7%	28.4%	370	0.0331	0.0574	11.9%	0.1792
1.0	15.4%	19.2%	370	0.0298	0.0225	−4.7%	0.1624
2.0	4.5%	7.3%	370	0.0181	0.0071	−16.2%	0.0792
			2-h lead time				
0.1	29.8%	40.5%	370	0.0340	0.0803	19.2%	0.1947
0.3	23.6%	30.0%	370	0.0207	0.0586	18.0%	0.1721
0.5	17.1%	23.2%	370	0.0276	0.0404	7.1%	0.1666
1.0	8.9%	15.1%	370	0.0313	0.0182	−10.0%	0.1439
2.0	2.0%	5.7%	370	0.0097	0.0065	−6.0%	0.0568

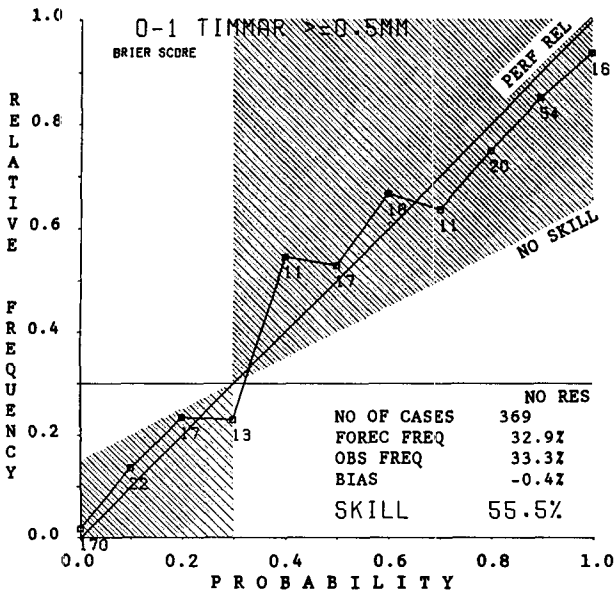

FIG. 4. Reliability diagram for forecasts of 1-h accumulated precipitation ≥0.5 mm, lead time 0 h. The forecast probability is on the X axis, and the observed frequency of hits is on the Y axis. Small squares with figures in the diagram give the number of cases. For instance, there were 20 forecasts giving the probability 0.8 (80%) of precipitation ≥0.5 mm. For 15 (75%) of these, precipitation ≥0.5 mm was observed (by conventional gages). Good forecasts are not only characterized by observations close to the line "perf rel" but also and mainly by having many observations far away from the point where the lines "perf rel" and "no res" cross. The shaded area marks skill > 0 compared to the climatological forecast, in this case a forecast of 30% probability for a rain amount ≥0.5 mm.

that establishing and managing a dense network of telemetering gages is costly, while a radar has an excellent resolution in space and time. For larger rain sums, no comparisons with persistency have been made. These forecasts have lower skill and with the present model it does not seem meaningful to make longer forecasts than 1 h for the threshold 1 mm or more.

5. Discussion and conclusions

The reason for the high skills is undoubtedly a sound physical basis for the method: the echoes generally move with the wind and during the first hour the distribution of reflectivities within the source area generally remains fairly constant and the source area is not too far away from the radar. For longer lead times the echo changes become more important; the source area may be so far away from the radar that the beam overshoots the precipitation and the skill decreases, but it is still positive for small rain sums after a lead time of two hours.

The forecasts have only been performed when rain was expected or there was rain in the area. This explains the high sample climatological probabilities. Running the forecasts continuously would result in a high number of "correct" forecasts of no risk for precipitation, contributing to higher scores. However, the climatological probabilities would be lower, which affects the skill scores adversely. Therefore, in routine work one should expect the method to give high scores similar to those obtained here, but not necessarily higher ones. What the scores really show is the skill decrease with lead time. Simple extrapolations like this one are nowcasting tools. The transformation from reflectivity to rainrate is known to give large errors. An alternative would have been to verify against accumulated precipitation according to the radar. This would probably give better scores, but we feel that verification against conventionally measured precipitation is fairer. Anomalous ground echoes are a problem for all works of this kind. Hitherto we have identified those echoes by manual inspection of the screen, but will introduce an algorithm for identifying them. Since there is a need for even shorter forecasts for sewer management and flood forecasting, we plan to test forecasts for shorter durations.

Acknowledgments. We want to thank Dr. Hans Alexandersson for valuable discussions.

TABLE 4. Skill parameters for probability forecasts of 1-h accumulated rain ≥0.1 mm for different lead times. Six rains 24 August–23 October 1989.

0 h			1 h			2 h		
Skill 1	Skill 2	Skill 3	Skill 1	Skill 2	Skill 3	Skill 1	Skill 2	Skill 3
60%	49%	21%	38%	24%	18%	19%	11%	9%

Skill 1 = Radar forecast with rounded sample climatology as reference.
Skill 2 = Persistency forecast with the same reference.
Skill 3 = Radar forecast with persistency as reference.

Skill 3 = 100 × (Skill 1 − Skill 2)/(100 − Skill 2)

Skill 3 gives an approximative value of the forecast skill compared with persistency forecast. Of course the values have uncertainties mostly because

A: Rounded sample climatology and "real" climatology are not equal.
B: Events with rain are much more common in the test period than in "real" climatology. The reason is that forecasts have only been made when rain is suspected.
C: There are few events in the test.

REFERENCES

Andersson, T., 1989: *An advective model for probability nowcasts of accumulated precipitation using radar.* Int. Symp. on Hydr. Appl. of Weather Radar, Univ. of Salford, 14–17.

Austin, G. L., A. Kilambi, A. Bellon, N. Leoutsarakos, A. Hausner, L. Trueman and M. Ivanich, 1986: Rapid II, an operational highspeed interactive analysis and display system for intensity radar data processing. Preprints, *23rd Conf. on Radar Meteorology,* Snowmass, Colorado, 79–82.

Brier, G. W., 1950: Verification of forecasts expressed in terms of probability, *Mon. Wea. Rev.,* **78,** 1–3.

Carpenter, K. M., and R. G. Owens, 1981: *Use of radar network data for forecasting rain.* COST 72 Workshop/Seminar on Weather Radar, 9–11 March, European Centre for Medium Range Weather Forecasts & The Meteorological Office Radar Research Laboratory, 159–182.

Cox, D. R., and H. D. Miller, 1980: *The Theory of Stochastic Processes.* Chapman and Hall, 5–16.

Einfalt, T., T. Denoeux and G. Jacquet, 1989: *The development of the scout II.0 rainfall forecasting method.* Int. Symp. on Hydr. Appl. of Weather Radar, Univ. of Salford, 14–17.

Gustafsson, N., and H. Törnevik, 1984: *Development of an Operational System for Very-Short-Range Forecasting (VSRF) at SMHI. Nowcasting II, Mesoscale Observations and Very-Short-Range Weather Forecasting. Proc. Second Int. Symp. on Nowcasting,* Norrköping, Sweden, 473–478.

Ivarsson, K-I., R. Joelsson, E. Liljas and A. H. Murphy, 1986: Probability Forecasting in Sweden: Some Results of Experimental and Operational Programs at the Swedish Meteorologial and Hydrological Institute. *Wea. Forecasting,* **1,** 136–154.

Murphy, A. H., and R. W. Katz, 1985: Probabilistic weather forecasting. *Probability, Statistics, and Decisions Making in the Atmospheric Sciences.* Westview Press, 337–377.

——, and H. Daan, 1984: Impact of feedback and experience on the quality of subjective weather forecasts: Comparison of results from the first and second years of the Zierikzee Experiment. *Mon. Wea. Rev.,* **112,** 413–423.

Persson, P. O. G., and T. Andersson, 1987: Automatic wind field interpretation of doppler radar radial wind components. PROMIS Reports No. 6, 72 p.

Walton, M. L., and E. R. Johnson, 1986: An improved precipitation projection procedure for the NEXRAD flash-flood potential system. *Preprints, 23rd Conf. on Radar Meteorology,* Snowmass, Colorado, 62–65.

Wickerts, S., 1982: Fine scale structures in time and space of rainfall rate. National Defence Research Institute, FOA report C 20448-E2, 79 p.

Zuckerberg, F. L., 1976: An application of the binomal distribution to radar observations for short-range precipitation forecasting. *Preprints, 6th Conf. on Weather Forecasting and Analysis,* 228–231.